Title

Magnetic Performance of the Advanced Light Source EPU5.0 Elliptically Polarizing Undulator

Permalink

https://escholarship.org/uc/item/0qn829rb

Authors

Marks, S
DeVries, J
Hoyer, E
et al.

Publication Date

1999-03-01

LBNL-43049

ERNEST ORLANDO LAWRENCE
BERKELEY NATIONAL LABORATORY

Magnetic Performance of the Advanced Light Source EPU5.0 Elliptically Polarizing Undulator

S. Marks, J. DeVries, E. Hoyer, B.M. Kincaid, D. Plate,
P. Pipersky, R.D. Schlueter, and A. Young

Advanced Light Source Division

March 1999

Presented at the
1999 Particle
Accelerator Conference,
New York, NY,
March 29–April 2, 1999,
and to be published in
the Proceedings

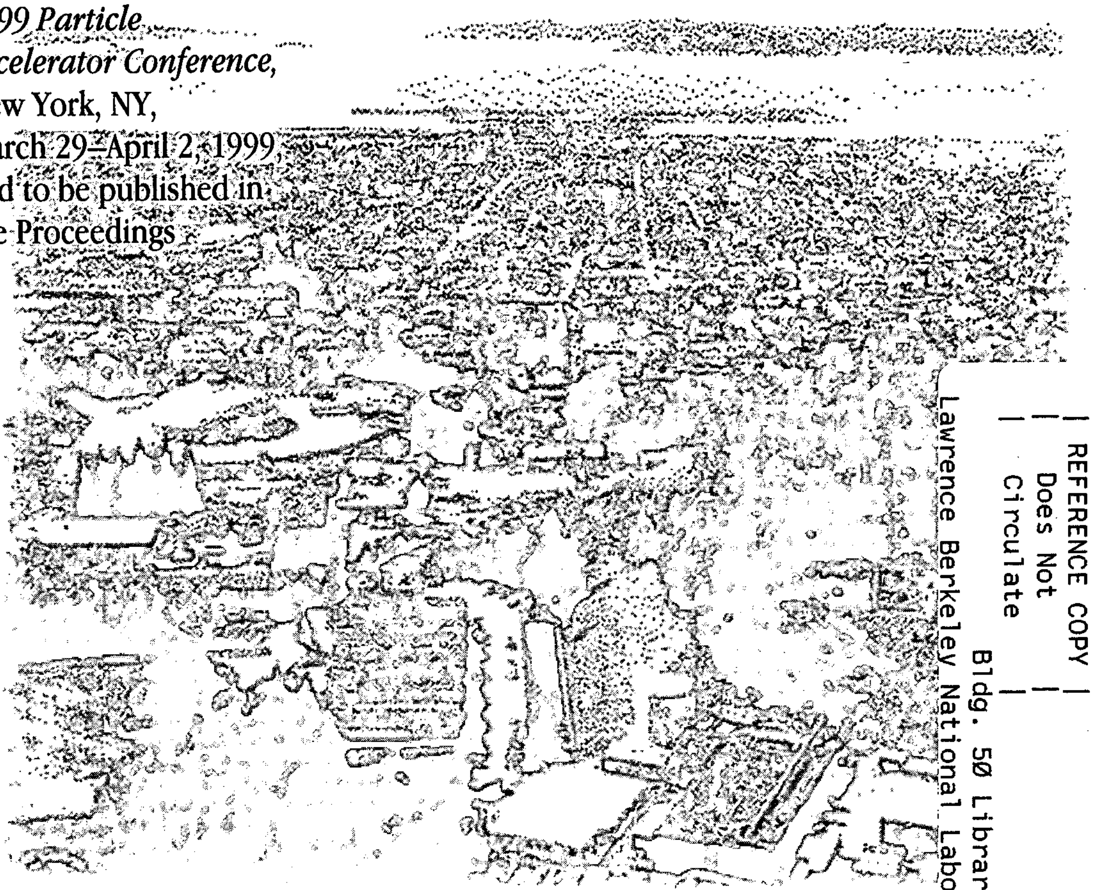

MAGNETIC PERFORMANCE OF THE ADVANCED LIGHT SOURCE EPU5.0 ELLIPTICALLY POLARIZING UNDULATOR

S. Marks, J. DeVries, E. Hoyer, B. M. Kincaid, D. Plate, P. Pipersky, R. D. Schlueter, A. Young,
Lawrence Berkeley National Laboratory, Berkeley, CA[*]

Abstract

An elliptically polarizing undulator (EPU) has been assembled, tested, and installed in the Advanced Light Source (ALS) storage ring. It is a 2 m long pure permanent magnet device with a 5.0 cm period capable of providing polarized radiation of any ellipticity. This paper reports on the program of magnetic measurements and field tuning, and final magnetic and drive system performance. A summary of measurement results, calculated radiation spectral performance, and a description of the magnetic shimming procedure used for field tuning are included.

1 INTRODUCTION

A facility dedicated for magnetic microscopy and spectroscopy is evolving at the ALS. This facility includes two undulator stations placed in tandem within a single storage ring straight.[1] A set of three chicane magnets separate the beams from the two devices by 2.53 mrad. The first undulator, an EPU5.0, the vacuum chambers and chicane are installed, have undergone accelerator tests and are operational.

The EPU design concept was first proposed by Sasaki.[2] The magnetic structure is a pure permanent magnet (PM) type including four identical quadrants. The diagonally juxtaposed quadrants, Q1 and Q3, are coupled and allowed to translate parallel to the axis. The other two quadrants, Q2 and Q4, are fixed. By moving Q1 and Q3 relative to Q2 and Q4, field amplitudes of B_x and B_y are modulated according to the following equations.

$$B_x = B_{x0}\sin(\varphi/2);\quad B_y = B_{y0}\cos(\varphi/2) \qquad (1)$$

B_{x0} and B_{y0} are peak amplitudes for the horizontal and vertical field components, respectively, and $\varphi = 2\pi dz/\lambda$, where dz corresponds to the quadrant shift and λ is the magnetic period. Regardless of relative magnitudes, the phase difference between B_x and B_y along the axis is 90°. When $dz = 0$ and $dz = \lambda/2$, $B_x = 0$ and $B_y = 0$, respectively, the electron trajectory is sinusoidal within a plane and the resulting radiation is linearly polarized in the horizontal and vertical planes, respectively. When $B_x = B_y$ the electron follows a helical trajectory and the resulting polarization is circular. For other values of dz, the polarization has intermediate ellipticities.

The helical mode produces on-axis radiation only in the fundamental. The brightness of radiation in higher harmonics is maximum for the linear polarized states. The EPU5.0 was designed to produce radiation with high brightness in the fundamental, and third and fifth harmonics with degrees of circular polarization exceeding 80%. The design photon energy range is 90 – 1500 eV for linear polarization, and 130 – 1500 eV for circular polarization.

2 MAGNETIC SHIMMING

Preparation for installation into the storage ring included an extensive program of drive system tests and magnetic measurements and field tuning. The magnetic field is adjusted by moving the vertically oriented PM blocks vertically and horizontally by up to ±0.25 mm with the use of mechanical shims.[1] The objectives of shimming are to correct local field errors that perturb the optical phase and to smooth nonuniformities in the lateral distribution of total field integrals, I_x and I_y.

2.1 Optical Phase Errors

The high brightness of an undulator depends upon the constructive interference of radiation along the electron trajectory. An accumulation of electron path deviations leads to phase errors that degrade the brightness. An expression for path length error $\Delta s(z)$ is shown below.

$$\begin{aligned}\Delta s(z) &= x_0(z)\Delta x'(z) + y_0(z)\Delta y'(z)\\ &\quad - \int_{-\infty}^{z}\left[x_0(\xi)\Delta x''(\xi) + y_0(\xi)\Delta y''(\xi)\right]d\xi \qquad (2)\\ &\quad + \frac{1}{2}\int_{-\infty}^{z}\left[\Delta x'^2(\xi) + \Delta y'^2(\xi)\right]d\xi\end{aligned}$$

The terms x_0 and y_0 are the unperturbed transverse coordinates, first and second derivatives correspond to velocity and magnetic field, respectively, and Δ indicates a perturbation due to field errors.

Two approaches have been used successfully to limit optical phase errors in conventional linear undulators. The first approach, as used in previous ALS hybrid devices, is to sufficiently limit RMS field errors[3] via application of appropriate magnet block and pole tolerances, and block sorting and placement. It is clear how this strategy works;

---

[*] Work supported by the Director, Office of Energy Research, Office of Basic Energy Sciences Division, U. S. Department of Energy, under Contract No. DE-A03-76SF00098.

all terms in Equation 2 are locally small, thus limiting the integral accumulation. The second approach, as exemplified in undulators built for ESRF, is to place iron shims within the magnetic structure to compensate for phase errors indicated by magnetic measurements.[4] The efficacy of this approach may be understood by examining Equation 2. While all errors make a positive definite contribution to the third term, local contributions to the first and second terms may be either positive or negative. The strategy followed in the placement of iron shims is to introduce field errors of the appropriate sign and location to cancel accumulated phase errors. In contrast to the first approach, this strategy generally increases RMS field errors.

Both of these approaches are problematic for application to an EPU. The absence of iron poles coupled with the achievable block-to-block variations in PM material naturally lead to relatively high field errors, before shimming. The iron-shimming scheme can be applied to compensate for phase errors corresponding to a single configuration of quadrant offset in the same way that works with a conventional undulator. However, upon changing the polarization state, via quadrant translation, the magnetic neighborhood of each shim, and thus its local on-axis magnetic effect, will change. Also, since shim placement generally does not correspond to field error locations, the efficacy of this approach depends critically upon the positions of initial field errors relative to those introduced by shims. This relationship changes with quadrant translation, since the shims' locations on one quadrant pair will shift relative to the errors belonging to the other quadrant pair. These considerations lead to the development of an alternative magnetic shimming approach.

The input to our magnetic shimming procedure was local magnetic field errors obtained from on-axis magnetic measurements at two polarizaiton states: horizontal linear polariztion, producing pure B_y on-axis, and vertical linear polarizaiton producing pure B_x on-axis. A constrained optimization procedure was applied to minimize an objective function composed of RMS values of local optical phase errors and local first field integrals for both polarization states. The variables within the optimization were the vertical and horizontal displacements of the vertically oriented PM blocks within each quadrant pair. Movements were constrained to ±0.25mm from initial locations. The effect of PM displacements was determined from analytically derived sensitivity coefficients.

2.2 Transverse Integral Nonuniformities

Local field adjustments to Q1 and Q3 are equivalent in how they affect on-axis fields and thus optical phase. However, the block movements used for field tuning also result in changes to the lateral distribution of field integrals, which are not symmetric about the axis. Therefore, Q1 and Q3 displacements are not equivalent in their effect on field integrals. Figure 1 shows perturbations in integral distributions due to vertical and horizontal magnet position adjustments of 0.25 mm in Q1. Adjustments to Q2, Q3, and Q4 are derived by applying appropriate symmetries.

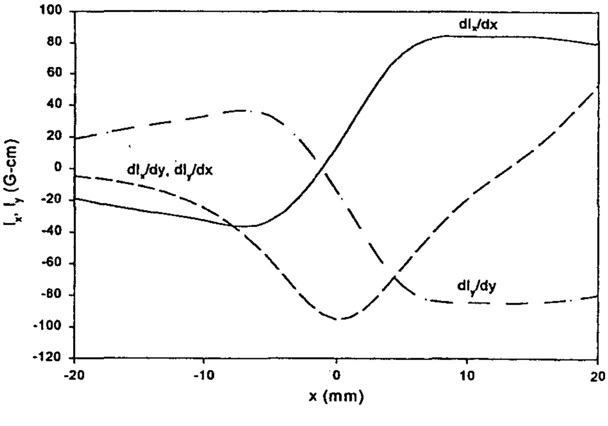

Figure 1 Change in I_x and I_y due to block motions *dx* and *dy* of 0.25 mm.

Our magnetic shimming procedure used the on-axis field optimization to identify PM block position adjustments for the Q1/Q3 and Q2/Q4 quadrant pairs. The choice between applying adjustments to Q1 or Q3, and Q2 or Q4 was made to minimize nonuniformities in lateral integral distributions.

2.2 Results of Magnetic Shimming

The RMS values, prior to shimming, for optical phase error and horizontal and vertical field integrals for the horizontal polarization mode were 10°, 147 G-cm and 95 G-cm, respectively. The values for vertical polarization were 32°, 218 G-cm, and 165 G-cm. After three tuning iterations, values for horizontal polariztion mode were reduced to 9°, 59 G-cm and 76 G-cm. The values for vertical polarization were 12°, 56 G-cm, and 64 G-cm. A fourth tuning iteration was applied for final integral adjustment. Figure 2 shows lateral integral distributions before and after shimming.

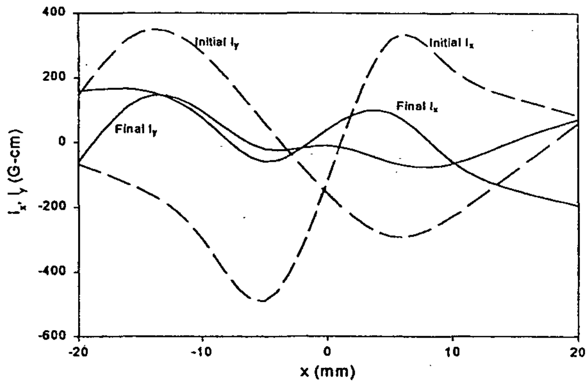

Figure 2 I_x and I_y, before and after magnetic tuning.

3 SPECTRAL CALCULATIONS

The magnetic shimming procedure used only field measurements for the two linear polarization states. Measurements were taken for other states to characterise performance over the operating range and provide assurance that optical phase errors had been adequately corrected over this range. Spectral properties were calculated done for a variety of polarization states. A computer code was developed that numerically integrates the full time domain electric field equations[5] for a single electron, without emittance and energy spread considerations.

Figure 3 summarises a comparison of spectral properties calculated from field measurements and from an error free device. The magnetic gap is 23 mm with a quadrant offset of 9 mm (an offset of 0 corresponds to the horizontal polarized configuration), corresponding to $B_y \approx 3B_x$, which produces a high degree of circular polarization with strong spectral brightness in the third and fifth harmonics. The third harmonic is at 660 eV, in the core energy range for many experiments.

Figure 3 illustrates the spectral effect due to magnetic field errors. The peak flux density ratio of the actual device (spectrum calculated from measured fields) to an ideal device (spectrum calculated from an error free device of the same magnetic structure) is graphed versus harmonic number. Notice that flux density is at or above 70% of ideal up to the ninth harmonic. Degree of circular polarization is also graphed as a function of harmonic number. In this configuration the degree of circular polarization is above 80% for all harmonics, and increases with harmonic number. Field errors do not degrade polarization.

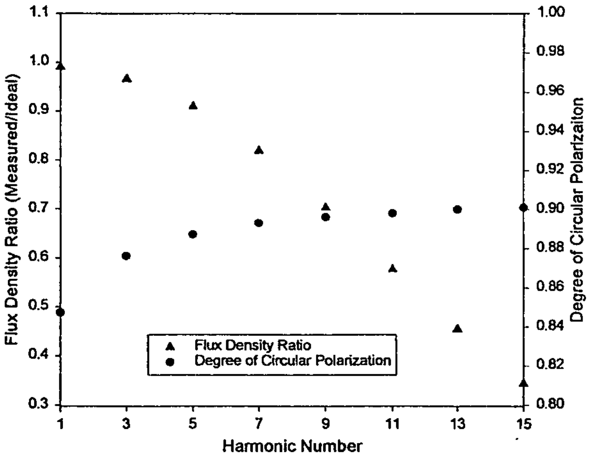

Figure 3 Flux density ratio and degree of circular polarization at 23 mm gap and 9 mm offset.

4 ON-AXIS FIELD INTEGRALS

Figure 4 shows the on-axis field integrals as a function of quadrant shift, *dz*, at the minimum gap of 14 mm. The change is due to the finite permeability of the PM and the change in proximity of end blocks to their neighbors. The effect on I_y is nearly canceled because the vertical magnetic structure is odd about the midpoint; the horizontal magnetic structure is even.

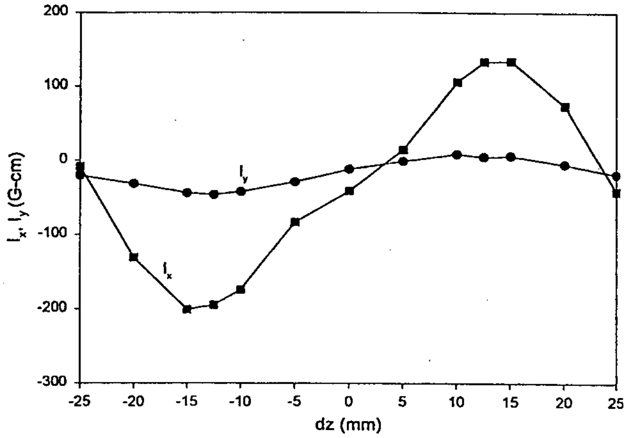

Figure 4 On-axis I_X and I_Y at 14 mm gap.

5 DRIVE SYSTEM ACCURACY

Very precise and repeatable control of the magnetic gap and quadrant translation is required to achieve the required precision and repeatability in spectral energy and degree of circular polarization.[6] The drive and motion control design has been described previously.[1]

Measurements demonstrated that final position repeatability was limited only by encoder resolution of 1 μm for vertical gap and 0.25 μm for quadrant offset. Settling time following a move was measured to be within 1.5 seconds.

6 REFERENCES

[1] S. Marks, et al., "The Advanced Light Source Elliptically Polarization Undulator," *Proc. 1997 Particle Accelerator Confernce* (1998) 3221.

[2] S. Sasaki, "Analyses for a planar variably-polarizing undulator", *Nucl. Instr. And Meth.* A347 (1994) 83.

[3] B. M. Kincaid, "Random errors in undulators and their effects on the radiation spectrum," *SPIE* Vol. 582 (1982) 72.

[4] J. Chavanne, P. Elleaume, "Undulator and wiggler shimming," *Synchrotron Radiation News* 8-1 (1995) 18.

[5] J. D. Jackson, *Classical Electrodynamics*, John Wiley & Sons (1975) 654.

[6] "EPU5.0 Elliptical Polarization Undulator Conceptual Design Report", to be published.

ERNEST ORLANDO LAWRENCE BERKELEY NATIONAL LABORATORY
ONE CYCLOTRON ROAD BERKELEY, CALIFORNIA 94720

Prepared for the U.S. Department of Energy under Contract No. DE-AC03-76SF00098